Computer Modeling in Engineering & Sciences

Tech Science Press

https://doi.org/10.32604/cmes.2026.083459 Published Online: 29 June 2026

ARTICLE

Bounded Data Modeling with the Extended Bradford Distribution: Modal Regression Approach and Applications

Emrah Altun[1,*], **Christophe Chesneau**[2] **and Atacan Erdis**[1]

[1]Department of Statistics, Gazi University, Ankara, Turkey
[2]Department of Mathematics, University of Caen-Normandie, Caen, France

*Corresponding Author: Emrah Altun. Email: emrahaltun123@gmail.com

Received: 04 April 2026; Accepted: 05 June 2026

ABSTRACT: Modeling bounded response variables is an important problem in computational statistics, especially in applications involving skewed, heavy-tailed data. In such cases, the modal regression is a robust alternative to traditional mean-based modeling approaches. In this study, a new bounded distribution, called the extended Bradford distribution, is proposed as a flexible extension of the classical Bradford distribution. By incorporating an additional shape parameter, the corresponding model can capture various shape structures, such as left and right skewness, increasing, and bathtub hazard shapes. The new distribution provides an explicit expression for the mode, making it suitable for modal regression. Based on this, a parametric modal regression model is developed, and parameter estimation is performed via the maximum likelihood method. The behavior of the estimators is investigated through comprehensive simulation studies. The practical usefulness of the proposed model is illustrated through applications, where the proposed model provides an improved fit compared to several competing models. In addition, an interactive R Shiny application is developed to facilitate the implementation, computation, and visualization of the model.

KEYWORDS: Bradford distribution; modal regression; residual; estimation; Mathematics Subject Classification: 62E15

1 Introduction

Regression analysis is a fundamental tool for examining the relationship between a set of explanatory variables and a response variable. The standard regression approaches focus on modeling the conditional expectation of the response variable, representing the central tendency of its association with the covariates. However, relying on the mean structure may be insufficient in practice, as such methods can lack robustness, particularly in datasets affected by outliers or characterized by heavy-tailed distributions (see [1,2]).

Models based on the conditional mode can provide a more useful representation of the underlying relationship than methods based on the conditional mean or median when the conditional distribution of the response variable given the covariates displays skewness or heavy tails. Reference [3] introduced two parametric modal regression models for bounded responses based on the beta distribution and provided diagnostic tools. Reference [4] presented a flexible parametric modal regression framework based on a heterogeneous Gumbel mixture distribution. Reference [5] developed a Bayesian modal regression using an unimodal distribution capable of accommodating symmetry, asymmetry, and varying tail behaviours through its shape and scale parameters. Reference [6] applied modal regression to neuroimaging data, demonstrating that traditional mean regression failed to capture meaningful associations due to the skewed and heavy-tailed nature of the cognitive assessment data. Reference [7] proposed three new modal regression

Copyright © 2026 The Authors. Published by Tech Science Press. This work is licensed under a Creative Commons Attribution 4.0 International License, which permits unrestricted use, distribution, and reproduction in any medium, provided the original work is properly cited.

models for bounded data based on unit-Gamma, kumaraswamy, and unit-Gompertz distributions, and showed that these models offer flexible and effective alternatives for modeling bounded responses under different data characteristics.

The primary motivation of this study arises from the increasing need for robust regression frameworks capable of effectively modeling bounded response variables in the presence of skewness, heavy tails, and outliers. While modal regression has recently gained attention as a robust alternative to mean-based approaches, its practical implementation remains limited due to the lack of suitable parametric distributions with analytically tractable modes.

Although several bounded distributions exist in the literature, most of them do not provide closed-form expressions for the mode, which restricts their applicability in a modal regression model (see [7]). Some of the recently proposed bounded distributions are examined. For instance, although the distribution of [8] is flexible, its mode cannot be obtained in closed form. The Poisson-unit-Weibull distribution of [9] is suitable for quantile regression, but it cannot be used for conditional mean and mode modeling of the response variable. Although the unit inverse exponentiated Lomax distribution of [10] is quite satisfactory at modeling various hazard forms, it lacks closed-form equations for mean and mode values. So, in the literature, many flexible distributions are available; however, their use in generalized linear models, time series, or engineering modeling is limited. Recently, Reference [11] introduced a one-parameter bounded distribution, called the Bradford distribution, with the following probability density function (pdf):

$$f(y) = \frac{\theta}{\log(\theta+1)(\theta y+1)}, \tag{1}$$

where $0 < y < 1$ and $\theta > 0$ is the scale parameter. While the Bradford distribution is notable for its simple, univariate structure, its use in modeling real-world datasets is quite limited. The Bradford distribution is right-skewed and has a monotonically increasing hazard rate function (hrf). In contrast, real-world datasets frequently exhibit different types of hrfs and left-skewness. To increase the flexibility of the Bradford distribution and improve its ability to model datasets with different characteristic structures, the extended Bradford (EB) distribution is proposed. The EB distribution can be used to model data that is skewed in both directions. It is also capable of modeling a variety of hrfs such increasing and bathtub. The EB distribution is suitable for modal regression models since its mode value has an explicit mathematical expression.

The proposed distribution differs from existing generalized bounded distributions in several important aspects. First, it preserves the analytical simplicity of the classical Bradford distribution while introducing an additional shape parameter that substantially increases flexibility. Second, the model is capable of modeling both left and right-skewed pdfs together with various hazard rate structures. Third, the mode of the distribution admits an explicit analytical expression, which enables a natural and computationally convenient reparameterization for modal regression purposes. These properties provide important practical advantages over several existing bounded models, including the beta and Kumaraswamy-based modal regression models. Therefore, the proposed approach offers flexibility, interpretability, and computational simplicity.

The presented study makes several key contributions to the literature. It introduces a new two-parameter bounded distribution that generalizes the classical Bradford distribution. It points out the key mathematical properties of the proposed distribution, including its moments, hazard rate behavior, and structural relationship with the beta distribution. It provides a closed-form expression for the mode, making the distribution particularly suitable for modal regression modeling. It develops a modal regression framework based on the EB distribution, including parameter estimation via maximum likelihood and diagnostic tools based on randomized quantile residuals. It implements the proposed model within an interactive R Shiny application, enhancing its accessibility and practical usability.

The rest of this paper is structured in the following way: In Section 2, the EB distribution is introduced, and its fundamental properties are presented. Section 3 is devoted to parameter estimation, where the maximum likelihood estimation procedure and its asymptotic properties are discussed along with a simulation study. In Section 4, the modal regression framework based on the EB distribution is developed, and the performance of the estimators is evaluated through Monte Carlo simulations. Section 5 illustrates the practical applicability of the model using real data examples, including both univariate and regression settings. In Section 6, an interactive implementation of the proposed method via an R Shiny application is described. Section 7 contains the limitations and possible future research.

2 Extended Bradford Distribution

Applying $X = Y^{\frac{1}{\alpha}}$ transformation where Y denotes a random variable with the pdf in (1), the pdf of the EB distribution is given by

$$f(x) = \frac{\alpha\theta x^{\alpha-1}}{\log(\theta+1)(\theta x^{\alpha}+1)}, \quad 0 < x < 1, \tag{2}$$

where $\alpha > 0$ is the shape parameter. The EB distribution reduces to the Bradford distribution for $\alpha = 1$. The cumulative distribution function (cdf) of the EB distribution is

$$F(x) = \frac{\log(1+\theta x^{\alpha})}{\log(1+\theta)}. \tag{3}$$

The quantile function (qf) of the EB distribution is

$$Q(p) = \left(\frac{(1+\theta)^{p}-1}{\theta}\right)^{\frac{1}{\alpha}}, \tag{4}$$

where $0 < p < 1$. The qf of the EB distribution is obtained in closed form. Therefore, the inverse transform method is easily implemented to generate random variables from the EB distribution. Fig. 1 shows the pdf shapes of the EB distribution according to different parameter values. The EB distribution stands out as a distribution that can be used to model extremely left or right-skewed data. The hrf of X is

$$h(x) = \frac{\alpha\theta x^{\alpha-1}}{(\log(1+\theta)-\log(1+\theta x^{\alpha}))(1+\theta x^{\alpha})}. \tag{5}$$

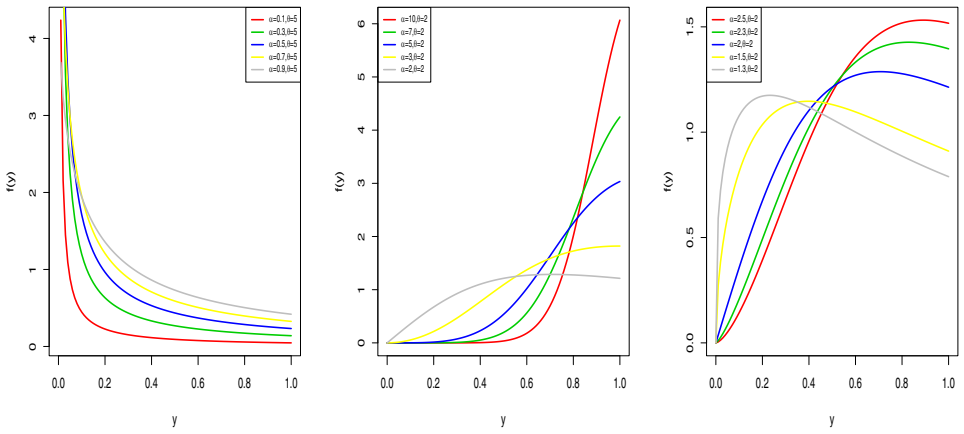


Figure 1: Pdf shapes of the EB distribution.

The hrf shapes of the EB distribution are displayed in Fig. 2. The distribution has two failure shapes: bathtub and increasing.

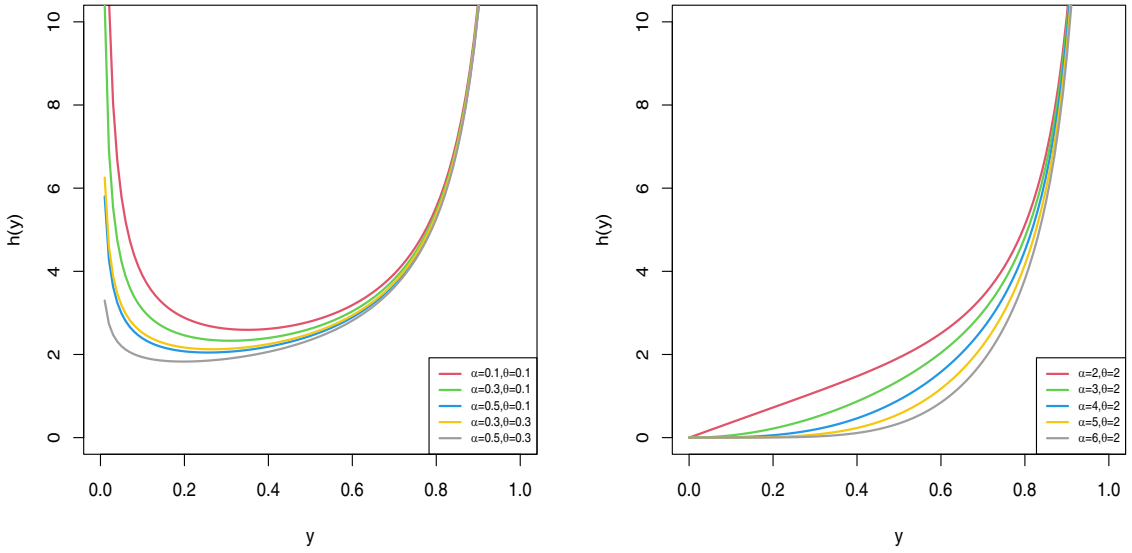


Figure 2: Hrf shapes of the EB distribution.

In the following subsection, the properties of the EB distribution are discussed in detail.

2.1 Connection with the Beta Distribution

The EB distribution has a structural connection with the beta distribution. The pdf of the beta distribution for $\beta = 1$ is

$$g(x) = \alpha x^{\alpha-1}, \quad 0 < x < 1. \tag{6}$$

The pdf of the proposed model can be rewritten as

$$f(x) = g(x)\frac{\theta}{\log(1+\theta)\,(\theta x^{\alpha}+1)}, \tag{7}$$

which reveals that the EB distribution can be interpreted as a weighted version of the Beta$(\alpha, 1)$ distribution. In this representation, the weighting function is

$$w(x) = \frac{1}{\theta x^{\alpha}+1}, \tag{8}$$

and $\log(1+\theta)/\theta$ is the normalizing constant. This representation shows that the proposed distribution belongs to the class of weighted distributions, where the baseline density is the Beta$(\alpha, 1)$ distribution and the weight function introduces additional flexibility in modeling skewness and tail behavior. Furthermore, as $\theta \to 0$,

$$f(x) \to \alpha x^{\alpha-1}, \tag{9}$$

which is the pdf of the Beta$(\alpha, 1)$ distribution.

2.2 Properties

Proposition 1. *The rth raw moment of X is*

$$E(X^r) = \frac{\theta\alpha}{\log(1+\theta)\,(\alpha+r)}\,{}_2F_1\left(1, 1+\frac{r}{\alpha}; 2+\frac{r}{\alpha}; -\theta\right), \tag{10}$$

where ${}_2F_1(\cdot)$ *denotes the Gauss hypergeometric function.*

Proof. The r-th raw moment is

$$E(X^r) = \int_0^1 x^r f(x;\alpha,\theta)\,dx. \tag{11}$$

Substituting the pdf in (11), we get

$$E(X^r) = \frac{\alpha\theta}{\log(1+\theta)} \int_0^1 \frac{x^{r+\alpha-1}}{1+\theta x^\alpha}\,dx. \tag{12}$$

Let $u = x^\alpha$, $du = \alpha x^{\alpha-1}dx$ and $x^{\alpha-1}dx = \frac{1}{\alpha}du$. Also, $x^{r+\alpha-1}dx = u^{\frac{r}{\alpha}}\frac{1}{\alpha}du$. Since $x \in (0,1)$, $u \in (0,1)$. Applying these substitution in (12), we have

$$E(X^r) = \frac{\theta}{\log(1+\theta)} \int_0^1 \frac{u^{\frac{r}{\alpha}}}{1+\theta u}\,du. \tag{13}$$

Let $\frac{r}{\alpha} = a-1$, the integral in (13) is

$$\int_0^1 \frac{u^{a-1}}{1+\theta u}.\,du. \tag{14}$$

Using the integral representation of the Gauss hypergeometric function, we obtain

$$\int_0^1 \frac{u^{a-1}}{1+\theta u}\,du = \frac{1}{a}\,{}_2F_1(1, a; a+1; -\theta). \tag{15}$$

Applying (15) in (13), the Eq. (13) becomes

$$E(X^r) = \frac{\theta}{\log(1+\theta)\alpha}\,{}_2F_1(1, a; a+1; -\theta). \tag{16}$$

Substituting $a = 1+\frac{r}{\alpha}$ in (16), we get

$$E(X^r) = \frac{\theta\alpha}{\log(1+\theta)\,(\alpha+r)}\,{}_2F_1\left(1, 1+\frac{r}{\alpha}; 2+\frac{r}{\alpha}; -\theta\right). \tag{17}$$

□

Proposition 2. *The mean of X is*

$$E(X) = \frac{\theta^{-1/\alpha}}{\log(1+\theta)}\,B_{\frac{\theta}{1+\theta}}\left(1+\frac{1}{\alpha}, -\frac{1}{\alpha}\right), \tag{18}$$

where $B_z(a,b)$ *denotes the incomplete beta function, given by [12].*

Proof. The mean of X is

$$E(X) = \int_0^1 x f(x)\, dx = \frac{\alpha\theta}{\log(1+\theta)} \int_0^1 \frac{x^{\alpha}}{1+\theta x^{\alpha}}\, dx. \tag{19}$$

Two transformations are used for the integration part of (19). First, let $u = x^{\alpha}, \quad du = \alpha x^{\alpha-1} dx$. Then, the integral becomes

$$E(X) = \frac{\theta}{\log(1+\theta)} \int_0^1 \frac{u^{1/\alpha}}{1+\theta u}\, du. \tag{20}$$

For the second transformation, let $y = \frac{\theta u}{1+\theta u}$, $u = \frac{y}{\theta(1-y)}$ and $du = \frac{1}{\theta(1-y)^2} dy$. When $u = 0$, $y = 0$; when $u = 1$, $y = \frac{\theta}{1+\theta}$. Substituting these change of variables in (20), we have

$$E(X) = \frac{\theta^{-1/\alpha}}{\log(1+\theta)} \int_0^{\frac{\theta}{1+\theta}} y^{1/\alpha}(1-y)^{-1/\alpha-1} dy. \tag{21}$$

The integral representation of the incomplete beta function is

$$B_x(a,b) = \int_0^x t^{a-1}(1-t)^{b-1} dt. \tag{22}$$

It is clear that the integration part in (21) is the incomplete beta function with the following parameters $x = \theta/(\theta+1)$, $a = 1/\alpha + 1$ and $b = -1/\alpha$. □

The expressions obtained in Propositions 1 and 2 are closely related. In Proposition 1, the rth raw moment of the EB distribution is expressed in terms of the Gauss hypergeometric function. In particular, setting $r = 1$ yields the mean of the distribution. On the other hand, in Proposition 2, the mean is expressed in terms of the incomplete beta function. Applying $y = \theta u/(1+\theta u)$ transformation in (15), we obtain

$$\begin{aligned} \int_0^1 \frac{u^{a-1}}{1+\theta u}\, du &= \theta^{-a} \int_0^{\frac{\theta}{1+\theta}} y^{a-1}(1-y)^{-a}\, dy \\ &= \theta^{-a} B_{\frac{\theta}{1+\theta}}(a, 1-a), \end{aligned} \tag{23}$$

which is the incomplete beta function representation of (15). Therefore, the expressions given in Propositions 1 and 2 are mathematically consistent. Using the similar approach in Proposition 2, the second raw moment of X is

$$E(X^2) = \frac{\theta^{-2/\alpha}}{\log(1+\theta)} B_{\frac{\theta}{1+\theta}}\left(1+\frac{2}{\alpha}, -\frac{2}{\alpha}\right). \tag{24}$$

So, the variance of X is

$$\mathrm{Var}(X) = \frac{\theta^{-2/\alpha}}{\log(1+\theta)} B_{\frac{\theta}{1+\theta}}\left(1+\frac{2}{\alpha}, -\frac{2}{\alpha}\right) - \left[\frac{\theta^{-1/\alpha}}{\log(1+\theta)} B_{\frac{\theta}{1+\theta}}\left(1+\frac{1}{\alpha}, -\frac{1}{\alpha}\right)\right]^2. \tag{25}$$

Proposition 3. *The moment generating function (mgf) of X is*

$$M_X(t) = \frac{\theta}{\log(1+\theta)} \sum_{k=0}^{\infty} \frac{t^k}{k!} \frac{1}{1+\frac{k}{\alpha}}\, {}_2F_1\left(1, 1+\frac{k}{\alpha}; 2+\frac{k}{\alpha}; -\theta\right). \tag{26}$$

Proof. The mgf is defined as

$$M_X(t) = \frac{\alpha\theta}{\log(1+\theta)} \int_0^1 \frac{x^{\alpha-1}e^{tx}}{1+\theta x^{\alpha}}\, dx. \tag{27}$$

Using the power series expansion for $\exp(tx) = \sum_{k=0}^{\infty} \frac{t^k x^k}{k!}$, the mgf is rewritten as

$$M_X(t) = \frac{\alpha\theta}{\log(1+\theta)} \sum_{k=0}^{\infty} \frac{t^k}{k!} \int_0^1 \frac{x^{k+\alpha-1}}{1+\theta x^{\alpha}}\, dx. \tag{28}$$

Using $u = x^{\alpha}$ transformation, we obtain

$$M_X(t) = \frac{\theta}{\log(1+\theta)} \sum_{k=0}^{\infty} \frac{t^k}{k!} \int_0^1 \frac{u^{\frac{k}{\alpha}}}{1+\theta u}\, du. \tag{29}$$

As in Proposition 1, the integral representation of the Gauss hypergeometric function can be used. Let $a = 1 + \frac{k}{\alpha}$, the integration part in (29) can be written as

$$\int_0^1 \frac{u^{a-1}}{1+\theta u}\, du = \frac{1}{a}\, {}_2F_1(1, a; a+1; -\theta). \tag{30}$$

Inserting (30) in (29), we get

$$M_X(t) = \frac{\theta}{\log(1+\theta)} \sum_{k=0}^{\infty} \frac{t^k}{k!} \frac{1}{a}\, {}_2F_1(1, a; a+1; -\theta). \tag{31}$$

Replacing $a = 1 + \frac{k}{\alpha}$ in (31), the mgf is

$$M_X(t) = \frac{\theta}{\log(1+\theta)} \sum_{k=0}^{\infty} \frac{t^k}{k!} \frac{1}{1+\frac{k}{\alpha}}\, {}_2F_1\left(1, 1+\frac{k}{\alpha}; 2+\frac{k}{\alpha}; -\theta\right). \tag{32}$$

□

Proposition 4. *If $\alpha \le 1$, the pdf is strictly decreasing on $(0,1)$ and the mode is at $x = 0$. If $\alpha > 1$, the pdf is unimodal and the mode is*

$$x^* = \left(\frac{\alpha-1}{\theta}\right)^{\frac{1}{\alpha}}, \tag{33}$$

where $(\alpha-1)/\theta < 1$. Otherwise the mode occurs at $x = 1$.

Proof. Since $\alpha > 0$ and $\theta > 0$, the normalizing constant $\frac{\alpha\theta}{\log(1+\theta)}$ does not affect the mode. Hence it is sufficient to maximize the below function to determine the mode of the EB distribution.

$$g(x) = \frac{x^{\alpha-1}}{1+\theta x^{\alpha}}. \tag{34}$$

The derivative of (34) is

$$g'(x) = \frac{x^{\alpha-2}\left[(\alpha-1) - \theta x^{\alpha}\right]}{(1+\theta x^{\alpha})^2}. \tag{35}$$

Since the denominator is strictly positive and $x^{\alpha-2} > 0$, the mode of the EB distribution is obtained by solving $(\alpha - 1) - \theta x^{\alpha} = 0$. So, the mode is

$$x^{*} = \left(\frac{\alpha - 1}{\theta}\right)^{\frac{1}{\alpha}}. \tag{36}$$

If $\alpha \leq 1$, then $(\alpha - 1) \leq 0$, so the equation has no positive solution in $(0,1)$. In this case, $g'(x) < 0$ for all $x \in (0,1)$ and the pdf is strictly decreasing; hence the mode is at $x = 0$.

If $\alpha > 1$, then $(\alpha - 1)/\theta > 0$, so a unique positive critical point exists. If $(\alpha + 1)/\theta < 1$, then $x^{*} \in (0,1)$ and this point yields the unique maximum since $g'(x)$ changes sign from positive to negative. If $\frac{\alpha-1}{\theta} \geq 1$, then the critical point lies outside the support, and $g'(x) > 0$ throughout $(0,1)$, so the pdf is increasing and the mode occurs at $x = 1$.

□

Proposition 5. *The EB distribution is log-convex for $\alpha \leq 1$.*

Proof. Consider the log-pdf of the EB distribution

$$\log f(x) = \log \alpha + \log \theta - \log\log(1 + \theta) + (\alpha - 1)\log x - \log(1 + \theta x^{\alpha}). \tag{37}$$

The second derivative of (37) with respect to x is

$$\frac{d^2}{dx^2}\log f(x) = -\frac{\alpha - 1}{x^2} - \frac{\theta\alpha x^{\alpha-2}\left[(\alpha - 1) - \theta x^{\alpha}\right]}{(1 + \theta x^{\alpha})^2}. \tag{38}$$

For $\alpha \leq 1$, we have

$$-\frac{\alpha - 1}{x^2} \geq 0, \qquad (\alpha - 1) - \theta x^{\alpha} < 0 \quad \forall x \in (0,1). \tag{39}$$

Hence the second term is positive, and we have

$$\frac{d^2}{dx^2}\log f(x) > 0, \quad \forall x \in (0,1). \tag{40}$$

Thus the log-pdf is convex, and the pdf is log-convex.

For $\alpha > 1$, the expression $(\alpha - 1) - \theta x^{\alpha}$ is positive for sufficiently small x and becomes negative for sufficiently large x. Therefore, the second derivative changes sign on $(0,1)$. Consequently, the log-pdf is neither concave nor convex on $(0,1)$.

□

Proposition 6. *The following results are obtained for the shape of the hrf:*

(i) *If $0 < \alpha < 1$, then $h(x)$ has a bathtub shape; that is, it is initially decreasing, attains a minimum, and then increases to infinity.*
(ii) *If $\alpha = 1$, then $h(x)$ is increasing on $(0,1)$.*
(iii) *If $\alpha > 1$, then $h(x)$ has a J-shape that starts from zero and goes to infinity.*

Proof. The hrf is given by

$$h(x) = \frac{\alpha\theta x^{\alpha-1}}{(1 + \theta x^{\alpha})\left[\log(1 + \theta) - \log(1 + \theta x^{\alpha})\right]}. \tag{41}$$

When $x \to 0^+$ and $x \to 1^-$, the limits of the hrf are given by

$$\lim_{x\to 0^+} h(x) = \begin{cases} \infty, & 0 < \alpha < 1, \\ \dfrac{\theta}{\log(1+\theta)}, & \alpha = 1, \\ 0, & \alpha > 1, \end{cases} \tag{42}$$

and

$$\lim_{x\to 1^-} h(x) = \infty. \tag{43}$$

Consider the derivative of $\log h(x)$, given by

$$\frac{d}{dx}\log h(x) = \frac{\alpha-1}{x} - \frac{\theta\alpha x^{\alpha-1}}{1+\theta x^{\alpha}}\left[1 + \frac{1}{\log(1+\theta) - \log(1+\theta x^{\alpha})}\right]. \tag{44}$$

The last term of (44) is strictly greater than 1 for all $x \in (0,1)$. The three cases are examined. The first case is for $0 < \alpha < 1$. As $x \to 0^+$, we have

$$\frac{\alpha-1}{x} \to -\infty.$$

So, we derive

$$\frac{d}{dx}\log h(x) < 0,$$

and $h(x)$ is decreasing near zero. As $x \to 1^-$, we have

$$\frac{d}{dx}\log h(x) \to -\infty,$$

and $h(x) \to \infty$. Since $h(x)$ first decreases and goes infinity, it has a bathtub shape $0 < \alpha < 1$.

The second case is for $\alpha = 1$. The hrf is

$$h(x) = \frac{\theta}{(1+\theta x)\left[\log(1+\theta) - \log(1+\theta x)\right]}. \tag{45}$$

Taking the first derivative of (45), we get

$$\frac{d}{dx}h(x) > 0 \quad \text{for all } x \in (0,1).$$

Hence, $h(x)$ is strictly increasing for $\alpha = 1$. The third case is for $\alpha > 1$. As $x \to 0^+$, we have $h(x) \to 0$ and

$$\frac{d}{dx}\log h(x) \sim \frac{\alpha-1}{x} > 0.$$

So, $h(x)$ increases near zero. As $x \to 1^-$, $h(x) \to \infty$. Therefore, $h(x)$ increases from zero to infinity. So, $h(x)$ has J-shaped for $\alpha > 1$.

□

Proposition 7. *The Rényi entropy of X is*

$$R_\delta(\alpha,\theta) = \frac{1}{1-\delta}\log\left[\frac{1}{\alpha}\left(\frac{\alpha\theta}{\log(1+\theta)}\right)^{\delta}\frac{1}{a}\,{}_2F_1(\delta,a;a+1;-\theta)\right], \tag{46}$$

where

$$a = \frac{\delta(\alpha-1)+1}{\alpha}.$$

Proof. The Rényi entropy is

$$R_\delta(\alpha,\theta) = \frac{1}{1-\delta}\log\left(\int_0^1 f(x)^\delta dx\right). \tag{47}$$

For the EB distribution, the integral part is

$$\int_0^1 f(x)^\delta dx = \left(\frac{\alpha\theta}{\log(1+\theta)}\right)^{\delta}\int_0^1 x^{\delta(\alpha-1)}(1+\theta x^\alpha)^{-\delta}dx. \tag{48}$$

Using $u = x^\alpha$ transformation, the integral is rewritten as follows:

$$\int_0^1 f(x)^\delta dx = \frac{1}{\alpha}\left(\frac{\alpha\theta}{\log(1+\theta)}\right)^{\delta}\int_0^1 u^{\frac{\delta(\alpha-1)+1}{\alpha}-1}(1+\theta u)^{-\delta}du. \tag{49}$$

As in Proposition 1, the integral in (49) can be expressed in terms of the Gauss hypergeometric function, as follows:

$$\int_0^1 u^{a-1}(1+\theta u)^{-\delta}du = \frac{1}{a}\,{}_2F_1(\delta,a;a+1;-\theta), \tag{50}$$

where

$$a = \frac{\delta(\alpha-1)+1}{\alpha}. \tag{51}$$

So, the Rényi entropy of X is

$$R_\delta(\alpha,\theta) = \frac{1}{1-\delta}\log\left[\frac{1}{\alpha}\left(\frac{\alpha\theta}{\log(1\theta)}\right)^{\delta}\frac{1}{a}\,{}_2F_1(\delta,a;a+1;-\theta)\right]. \tag{52}$$

□

For a detailed shape analysis of the EB distribution, its skewness and kurtosis values are obtained via computational implementation of the Gauss hypergeometric function in the gsl package of R. The computational results in Fig. 3 indicate that an increase in α leads to a decrease in both skewness and kurtosis, whereas an increase in θ yields the opposite effect.

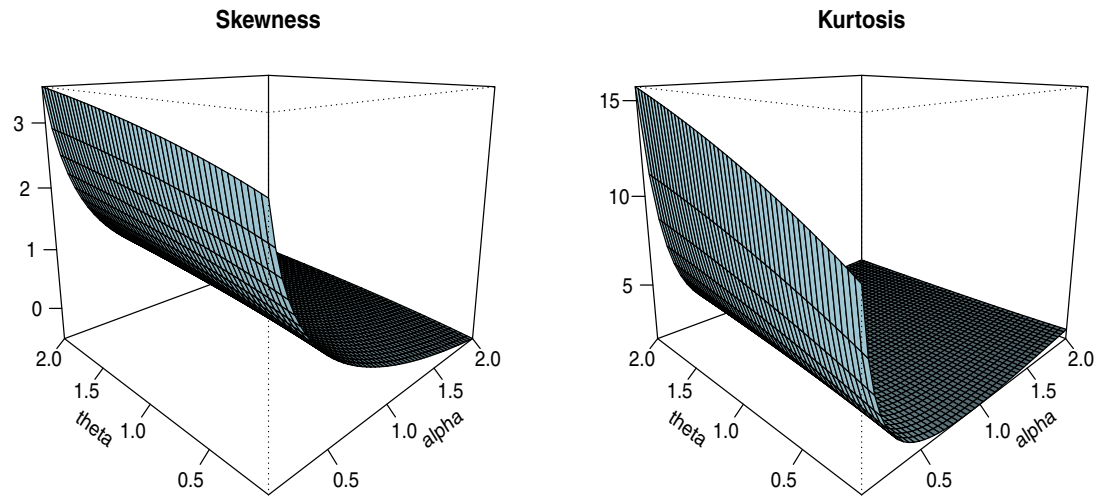


Figure 3: Skewness and kurtosis values of the EB distribution.

3 Estimation

The parameter estimation for the EB distribution via the maximum likelihood estimation (MLE) method is detailed in this section. Furthermore, the asymptotic efficiency of the ML estimators is evaluated through a comprehensive simulation study.

3.1 Maximum Likelihood

The log-likelihood function of the EB distribution is

$$\ell(\alpha,\theta) = n\log\alpha + n\log\theta + (\alpha-1)\sum_{i=1}^{n}\log x_i - n\log\log(1+\theta) - \sum_{i=1}^{n}\log(1+\theta x_i^{\alpha}). \tag{53}$$

Differentiating (53) with respect to α and θ, we obtain

$$\frac{\partial\ell}{\partial\alpha} = \frac{n}{\alpha} + \sum_{i=1}^{n}\log x_i - \sum_{i=1}^{n}\frac{\theta x_i^{\alpha}\log x_i}{1+\theta x_i^{\alpha}}, \tag{54}$$

$$\frac{\partial\ell}{\partial\theta} = \frac{n}{\theta} - \frac{n}{(1+\theta)\log(1+\theta)} - \sum_{i=1}^{n}\frac{x_i^{\alpha}}{1+\theta x_i^{\alpha}}. \tag{55}$$

The ML estimators $(\hat{\alpha},\hat{\theta})$ are obtained by solving the following nonlinear system:

$$\frac{\partial\ell}{\partial\alpha} = 0, \qquad \frac{\partial\ell}{\partial\theta} = 0.$$

Since these equations involve nonlinear terms, the closed-form solutions do not exist. Therefore, iterative optimization algorithms should be employed. The elements of the observed information matrix are given by

$$I_{(\alpha,\alpha)} = \frac{\partial^2\ell}{\partial\alpha^2} = -\frac{n}{\alpha^2} - \sum_{i=1}^{n}\frac{\theta x_i^{\alpha}(\log x_i)^2}{(1+\theta x_i^{\alpha})^2}, \tag{56}$$

$$I_{(\theta,\theta)} = \frac{\partial^2 \ell}{\partial \theta^2} = -\frac{n}{\theta^2} + \frac{n\left[(1+\theta)\log(1+\theta) - 1\right]}{(1+\theta)^2 \log^2(1+\theta)} - \sum_{i=1}^{n} \frac{x_i^{2\alpha}}{(1+\theta x_i^{\alpha})^2}, \tag{57}$$

$$I_{(\alpha,\theta)} = \frac{\partial^2 \ell}{\partial \alpha \partial \theta} = -\sum_{i=1}^{n} \frac{x_i^{\alpha} \log x_i}{(1+\theta x_i^{\alpha})^2}. \tag{58}$$

When the standard regularity conditions hold, the MLEs for the EB distribution are consistent and asymptotically normal. Let $\Theta = \{(\alpha, \theta) : \alpha > 0, \theta > 0\}$ be the parameter space. Given that the support of the distribution is parameter-independent and its log-likelihood function is twice continuously differentiable with respect to (α, θ), the regularity conditions are satisfied. Moreover, model identifiability is ensured since distinct parameter vectors result in distinct PDFs. Therefore, based on classical likelihood theory, it follows that

$$\sqrt{n}\begin{pmatrix} \hat{\alpha} - \alpha \\ \hat{\theta} - \theta \end{pmatrix} \xrightarrow{d} N_2\left(0, I(\alpha, \theta)^{-1}\right).$$

3.2 Simulation

The performance of the MLEs in terms of bias, mean squared error (MSE), and mean relative error (MRE) is discussed under different sample sizes and parameter vectors. The simulation is repeated 1000 times. The used parameter vectors are $(\alpha = 2, \theta = 2)$, $(\alpha = 0.5, \theta = 0.5)$, and $(\alpha = 1.5, \theta = 0.5)$.

The simulation results given in Table 1 reveal clear and consistent results for all parameter settings. As the sample size increases from $n = 100$ to $n = 5000$, all performance measures improve substantially. Specifically, the bias of both $\hat{\alpha}$ and $\hat{\theta}$ decreases monotonically toward zero, indicating that the estimators are asymptotically unbiased. Similarly, the MSE values decrease significantly with increasing sample size, confirming the consistency of the MLEs. Moreover, the MRE values approach 1 as n increases, suggesting that the estimators become increasingly accurate in relative terms.

Table 1: Simulation results of the EB distribution for three parameter vectors.

Sample Sizes	True Values	$\alpha = 2$	$\theta = 2$	$\alpha = 0.5$	$\theta = 0.5$	$\alpha = 1.5$	$\theta = 0.5$
	Metrics	α	θ	α	θ	α	θ
100	Bias	0.0534	0.7537	0.0349	0.7288	0.1069	0.6966
	MSE	0.0960	3.9448	0.0092	2.8448	0.0807	2.5554
	MRE	1.0267	1.3768	1.0699	2.4576	1.0712	2.3933
500	Bias	0.0208	0.2762	0.0069	0.1368	0.0212	0.1596
	MSE	0.0285	1.2336	0.0020	0.3255	0.0162	0.3162
	MRE	1.0104	1.1381	1.0138	1.2736	1.0142	1.3192
1000	Bias	0.0109	0.1508	0.0014	0.0557	0.0078	0.0567
	MSE	0.0163	0.7011	0.0011	0.1740	0.0089	0.1304
	MRE	1.0054	1.0754	1.0028	1.1114	1.0052	1.1134
5000	Bias	0.0039	0.0332	0.0009	0.0160	0.0025	0.0160
	MSE	0.0032	0.1206	0.0002	0.0235	0.0019	0.0247
	MRE	1.0019	1.0166	1.0017	1.0321	1.0017	1.0319

A notable difference is observed between the estimation performance of α and θ. The estimator of α performs considerably better across all scenarios, exhibiting smaller bias, lower MSE, and MRE values very close to 1 even for relatively small sample sizes. In contrast, the estimator of θ shows substantially higher bias and MSE, particularly when $n = 100$. Additionally, the MRE values for θ are significantly larger than 1 in small samples, indicating poor relative accuracy. This suggests that θ is more difficult to estimate and may be more sensitive to sampling variability. Therefore, bias-reduction techniques or alternative estimation methods should be considered.

Note that all computations are conducted in the R software. The MLEs are obtained using the optim function with the Nelder-Mead optimization algorithm. To improve numerical stability and reduce sensitivity to initial values, multiple starting values are considered in the optimization procedure. The observed information matrix is numerically evaluated at the MLEs of the EB distribution and used to compute standard errors and asymptotic confidence intervals. Throughout the simulation experiments, the convergence is achieved in almost all replications.

4 Modal Regression

The mode of the EB distribution is (for $\alpha > 1$)

$$x^* = \left(\frac{\alpha - 1}{\theta}\right)^{\frac{1}{\alpha}}. \tag{59}$$

The EB distribution is re-parametrized by means of the its mode. Let $\theta = (\alpha - 1)\,\mu^{-\alpha}$, the pdf of the mode-parametrized EB distribution is

$$f(y) = \frac{\alpha\,(\alpha - 1)\,\mu^{-\alpha}\,y^{\alpha-1}}{\log\left((\alpha - 1)\,\mu^{-\alpha} + 1\right)\left((\alpha - 1)\,\mu^{-\alpha}\,y^{\alpha} + 1\right)}. \tag{60}$$

The pdf in (60) is denoted as EB (μ, α), where $\alpha > 0$, $\mu \in (0,1)$, and mode $(Y) = \mu$. The shapes of the pdf in (60) are displayed in Fig. 4.

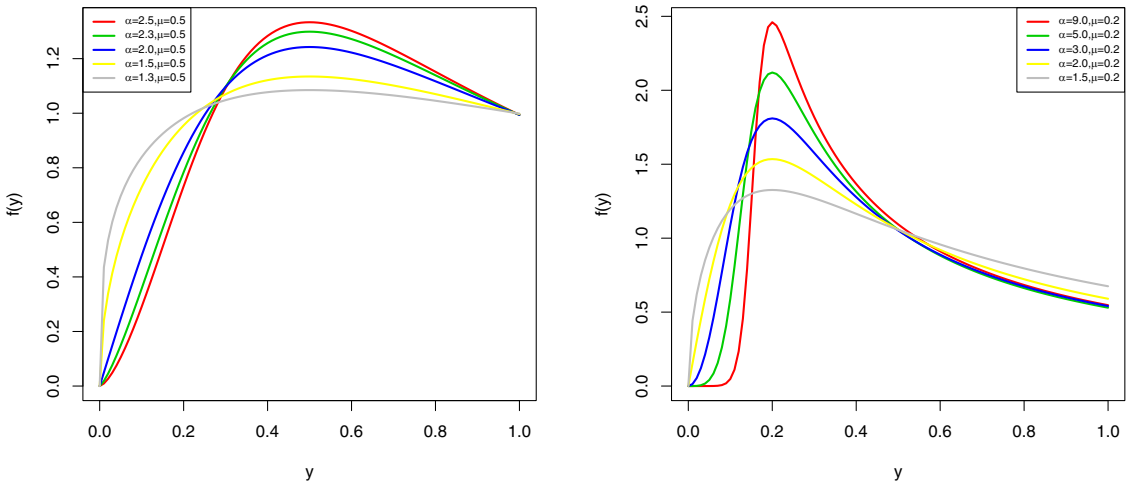


Figure 4: Pdf shapes of the mode-parametrized EB distribution.

Let y_i, $i = 1, 2, \ldots, n$ be the realizations of the random variable with the pdf in (60). The conditional mode of the parametrized EB distribution is modeled with the logit link function

$$\mu_i = \frac{\exp\left(\mathbf{x}_i \boldsymbol{\gamma}^T\right)}{1 + \exp\left(\mathbf{x}_i \boldsymbol{\gamma}^T\right)}, \tag{61}$$

where $\boldsymbol{\gamma} = \left(\gamma_0, \gamma_1, \gamma_2, \ldots, \gamma_p\right)^T$ is unknown regression parameter vector and $\mathbf{x}_i = \left(1, x_{i1}, x_{i2}, x_{i3}, \ldots, x_{ip}\right)^T$ is the i^{th} vector of known covariates. Since the mode of the EB distribution is within the range of (0, 1), the logit link function is used.

Substituting the link function (61) in (60), the log-likelihood function of the EB modal regression is

$$\begin{aligned}\ell\left(\boldsymbol{\gamma}, \alpha\right) &= n \log\left(\alpha\left(\alpha - 1\right)\right) - \alpha \sum_{i=1}^{n} \log\left(\mu_i\right) + \left(\alpha - 1\right) \sum_{i=1}^{n} \log\left(y_i\right) \\ &- \sum_{i=1}^{n} \log\left(\log\left(\left(\alpha - 1\right) \mu_i^{-\alpha} + 1\right)\right) + \sum_{i=1}^{n} \log\left(\left(\alpha - 1\right) \mu_i^{-\alpha} y_i^{\alpha} + 1\right),\end{aligned} \tag{62}$$

where μ_i is defined in (61). As expected, there is no explicit solution for the ML estimators of $(\boldsymbol{\gamma}, \alpha)$. For this reason, direct maximization of (62) is required to obtain $(\hat{\boldsymbol{\gamma}}, \hat{\alpha})$. There are many available packages in several software to maximize the likelihood function. Here, the optim function in R is preferred. Based on the observed information matrix, the standard errors and asymptotic confidence intervals of the parameters are constructed. The model accuracy is evaluated by the randomized quantile residual (see [13])

$$r_i = \Phi^{-1}\left(p_i\right),$$

where $p_i = F_{\hat{\mu}_i, \hat{\alpha}}\left(y_i\right)$ and Φ^{-1} is the qf of the $\mathrm{N}\left(0, 1\right)$ distribution. When the fitted model adequately captures the data, r_i follows the $\mathrm{N}\left(0, 1\right)$ distribution.

4.1 Simulation of EB Modal Regression Model

The asymptotic behavior of the ML estimates for the EB modal regression model is investigated through a Monte Carlo simulation study. The dependent variable is generated using the logit link function defined as

$$\operatorname{logit}\left(\mu_i\right) = \gamma_0 + \gamma_1 x_{i1} + \gamma_2 x_{i2}. \tag{63}$$

Note that μ_i in (63) can be rewritten as in (61). Two different parameter settings are considered:

- Case I: $\gamma_0 = -2, \gamma_1 = -1, \gamma_2 = 0.5, \alpha = 2$,
- Case II: $\gamma_0 = -3, \gamma_1 = 1.5, \gamma_2 = -1.5, \alpha = 2$.

The covariates x_{i1} and x_{i2} are independently generated from the standard uniform distribution. For each configuration, the simulation is replicated 1000 times. The performance of the ML estimators is evaluated in terms of the empirical mean, bias, and MSE, and the results are reported in Table 2.

The results indicate that the ML estimators perform satisfactorily in both scenarios. As the sample size increases, the empirical means of the estimates approach the true parameter values, demonstrating consistency. The bias values are relatively small even for moderate sample sizes and tend to decrease as n increases.

Moreover, the MSE values exhibit a clear decreasing pattern with increasing sample size, confirming the efficiency of the estimators. This behavior is observed consistently across all parameters in both Case I and Case II. In particular, the estimation of the shape parameter α shows relatively larger bias and MSE for

smaller sample sizes; however, its performance improves significantly as the sample size grows. In summary, these numerical findings offer robust empirical support for the consistency and asymptotic efficiency of the parameter estimates in the EB modal regression model.

Table 2: Simulation results of the EB modal regression model.

n	EM	I				II			
		$\gamma_0 = -2$	$\gamma_1 = -1$	$\gamma_2 = 0.5$	$\alpha = 2$	$\gamma_0 = -3$	$\gamma_1 = 1.5$	$\gamma_2 = -1.5$	$\alpha = 2$
100	Mean	−2.0258	−0.9612	0.5075	2.2322	−2.9965	1.5032	−1.4996	2.2790
	Bias	−0.0258	0.0388	0.0075	0.2322	0.0035	0.0032	0.0004	0.2790
	MSE	0.2545	0.4094	0.4605	0.4366	0.2067	0.4073	0.4021	0.4168
250	Mean	−2.0030	−1.0008	0.5152	2.1380	−3.0083	1.4995	−1.4894	2.1387
	Bias	−0.0030	−0.0008	0.0152	0.1380	−0.0083	−0.0005	0.0106	0.1387
	MSE	0.1496	0.2607	0.2404	0.1482	0.1625	0.2577	0.2603	0.1980
500	Mean	−1.9954	−0.9945	0.4917	2.0474	−2.9888	1.5169	−1.5230	2.0705
	Bias	0.0046	0.0055	−0.0083	0.0474	0.0112	0.0169	−0.0230	0.0705
	MSE	0.0688	0.1166	0.1257	0.0562	0.0647	0.1236	0.1206	0.0693
1000	Mean	−2.0070	−0.9987	0.5173	2.0265	−2.9945	1.5030	−1.5021	2.0342
	Bias	−0.0070	0.0013	0.0173	0.0265	0.0055	0.0030	−0.0021	0.0342
	MSE	0.0340	0.0610	0.0627	0.0265	0.0361	0.0593	0.0574	0.0280

5 Applications

5.1 Univariate Case

Reference [14] introduced the log-cosine-power (LCP) distribution and demonstrated its flexibility using a real data set on failure times. This data set, originally analyzed in [14], has also been considered in comparison with several competing unit distributions, including the unit Teissier distribution [15], transmuted unit Rayleigh distribution [16], Topp-Leone distribution [17], unit-exponential distribution [18], and unit Burr XII distribution [19]. According to [14], the LCP distribution provides the best fit among these models, as evidenced by the lowest Akaike information criterion (AIC) and Bayesian information criterion (BIC) values, along with the highest p-value of the Kolmogorov-Smirnov (KS) test. Specifically, the reported AIC, BIC, and p-value for the LCP model are −7.0748, −3.1721, and 0.5635, respectively.

In this study, the same data set is reanalyzed to assess the performance of the proposed EB distribution in (2), and compared with well-known alternative models. The competing models considered are the beta and Kumaraswamy (Kum) [20] models. The estimation results and goodness-of-fit statistics are presented in Table 3.

The results indicate that the EB model outperforms the competing models. In particular, it yields the smallest AIC and BIC values. Furthermore, the EB model produces the lowest KS statistic and the highest corresponding p-value, providing strong evidence that it offers the closest agreement with the empirical distribution of the data.

Table 3: Comparison of the EB distribution with the beta and Kum distributions.

Models	α	β	$-\ell$	AIC	BIC	KS	p-value
Beta(α, β)	0.6775 0.1107	1.0412 0.1873	−5.6714	−7.3427	−3.2218	0.1038	0.5600
Kum(α, β)	0.6825 0.1145	1.0472 0.1794	−5.6824	−7.3648	−3.2439	0.1035	0.5631
EB(α, β)	0.8373 0.2666	1.7366 3.7457	−5.9766	−7.9533	−3.8324	0.0970	0.6467

The graphical analysis presented in Fig. 5 provides additional support in favour of the EB distribution. The fitted PDF of the EB distribution is close to the empirical histogram and successfully captures both the central tendency and the tail behavior. Overall, both the numerical and graphical findings provide adequate evidence that the EB distribution offers a more flexible and accurate modeling for the considered failure time data.

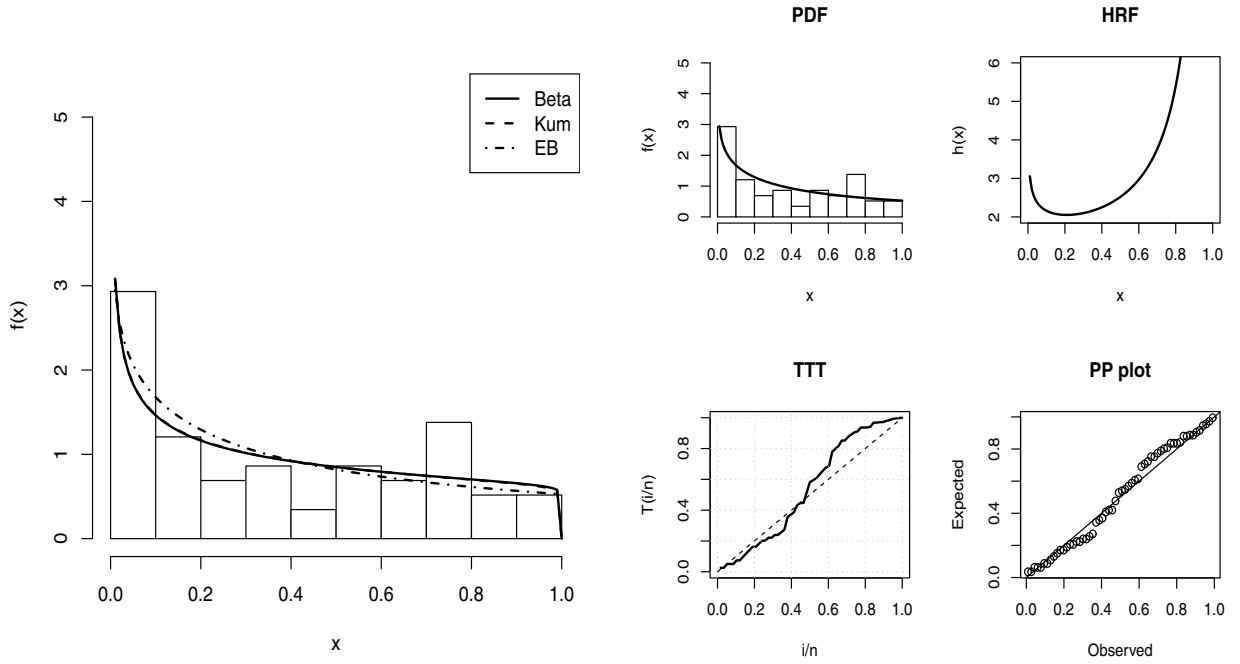


Figure 5: Fitted pdfs of the considered models.

5.2 Regression with Covariates

The water quality (WQ) indicator of the OECD (Organisation for Economic Co-operation and Development) countries is modelled with the air pollution (AP) and long-term unemployment rate (LTUR) indicators. The EB modal regression model is compared with the beta and gamma modal regression models. The results are reported in Table 4.

Table 4: Modal regression results.

Covariates	Beta			Gamma			EB		
	EST	SE	*p*-value	EST	SE	*p*-value	EST	SE	*p*-value
Constant	3.1979	0.6188	<0.0001	2.7211	0.4943	<0.0001	1.3130	0.4625	0.0045
AP	−0.1218	0.0333	0.0002	−0.0942	0.0332	0.0050	−0.0826	0.0212	<0.0001
LTUR	−0.3880	0.1390	0.0050	−0.3068	0.1375	0.0260	−0.1786	0.0317	<0.0001
Dispersion	1.8860			2.2055			24.1119		
$-\ell$	−19.9450			−13.3275			−20.3408		
AIC	−31.8900			−18.6550			−32.6816		
BIC	−25.6690			−22.7290			−26.4602		

EST: Estimate, SE: Standard error

The coefficient of AP is negative and statistically significant for all fitted models. It indicates that higher levels of AP are associated with lower levels of WQ. In other words, an increase in AP leads to a deterioration in WQ, which is consistent with environmental theory and empirical expectations. Similarly, the LTUR exhibits a negative and significant effect on WQ in all models. It suggests that higher unemployment rates are linked to poorer environmental outcomes, possibly reflecting reduced public and private investment in environmental protection. Overall, the estimated coefficients provide consistent evidence that both environmental and socio-economic factors play a crucial role in determining WQ for OECD countries.

Additionally, it can be seen that the EB modal regression model has lower AIC and BIC values than the other two models. Therefore, the EB model yields better results than the beta and gamma modal regression models for this dataset.

The results of the KS test, applied to the randomized quantile residuals of the fitted regression models, are presented in Table 5. The residuals obtained from all fitted models follow a standard normal distribution. However, the *p*-value obtained for the EB model is higher than that of the other two models.

Table 5: KS test results for the residuals.

Models	Statistics	*p*-value
Beta	0.2027	0.0973
Gamma	0.0973	0.8630
EB	0.0856	0.9402

Fig. 6 shows the quantile-quantile (QQ) plot for the residuals. It is worth noting that the theoretical quantile values in the QQ plot obtained for the EB model are closer to the empirical values than those for the other two models.

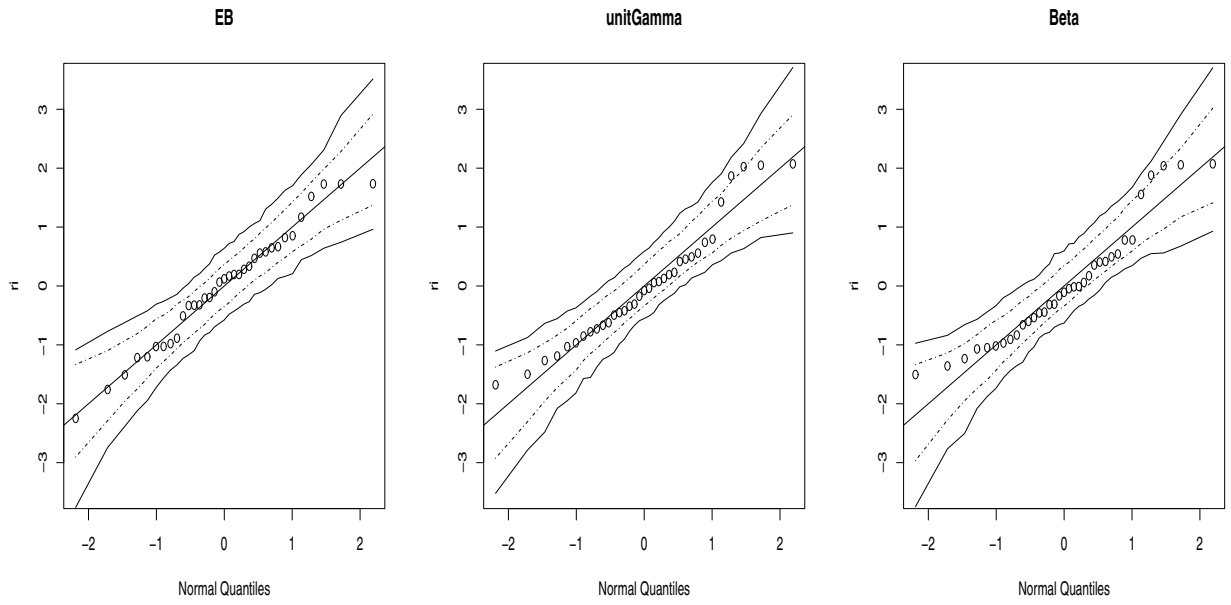


Figure 6: QQ plots of the residuals.

6 Implementation of EB Modal Regression Model via R Shiny

An interactive web-based application is developed using the R Shiny framework to facilitate the implementation of the proposed model. The application, available at https://gazistat.shinyapps.io/EBMR/, is designed to provide an accessible and user-friendly environment for performing estimation, model evaluation, and diagnostic analysis of the EB model.

The interface is structured into four main panels: *Data*, *Regression*, *Diagnostics*, and *Univariate Fit*. Each panel is designed to guide the user through a specific stage of the analysis.

The *Data* panel allows users to upload datasets in commonly used formats such as `.csv` and `.xlsx` (see Fig. 7). Within this panel, users can select the dependent and independent variables and identify categorical covariates. For categorical variables, the application enables the specification of reference levels, ensuring proper model interpretation. In addition, a validation mechanism checks whether the dependent variable lies within the unit interval and provides a warning if the condition is violated.

The *Regression* panel presents the results obtained from the estimation procedure (see Fig. 8). It reports parameter estimates along with their standard errors, test statistics, and significance levels. Furthermore, commonly used model selection criteria is provided to support model comparison and evaluation.

The *Diagnostics* panel is devoted to assessing model adequacy (see Fig. 9). It provides graphical and numerical tools based on randomized quantile residuals. In particular, the QQ plot is displayed to visually evaluate the agreement between empirical and theoretical distributions. In addition, the KS test is reported to assess the goodness-of-fit. The panel also allows users to export the diagnostic plot in PDF and EPS formats for reporting purposes.

The *Univariate Fit* panel enables users to fit the proposed distribution to univariate data (see Fig. 10). Users can upload a dataset, select a variable, and specify initial parameter values. The panel reports parameter estimates, information criteria, and goodness-of-fit measures. It also provides graphical outputs, including fitted density curves, hrfs, survival functions, and probability plots, which help to visually assess the adequacy of the fitted distribution.

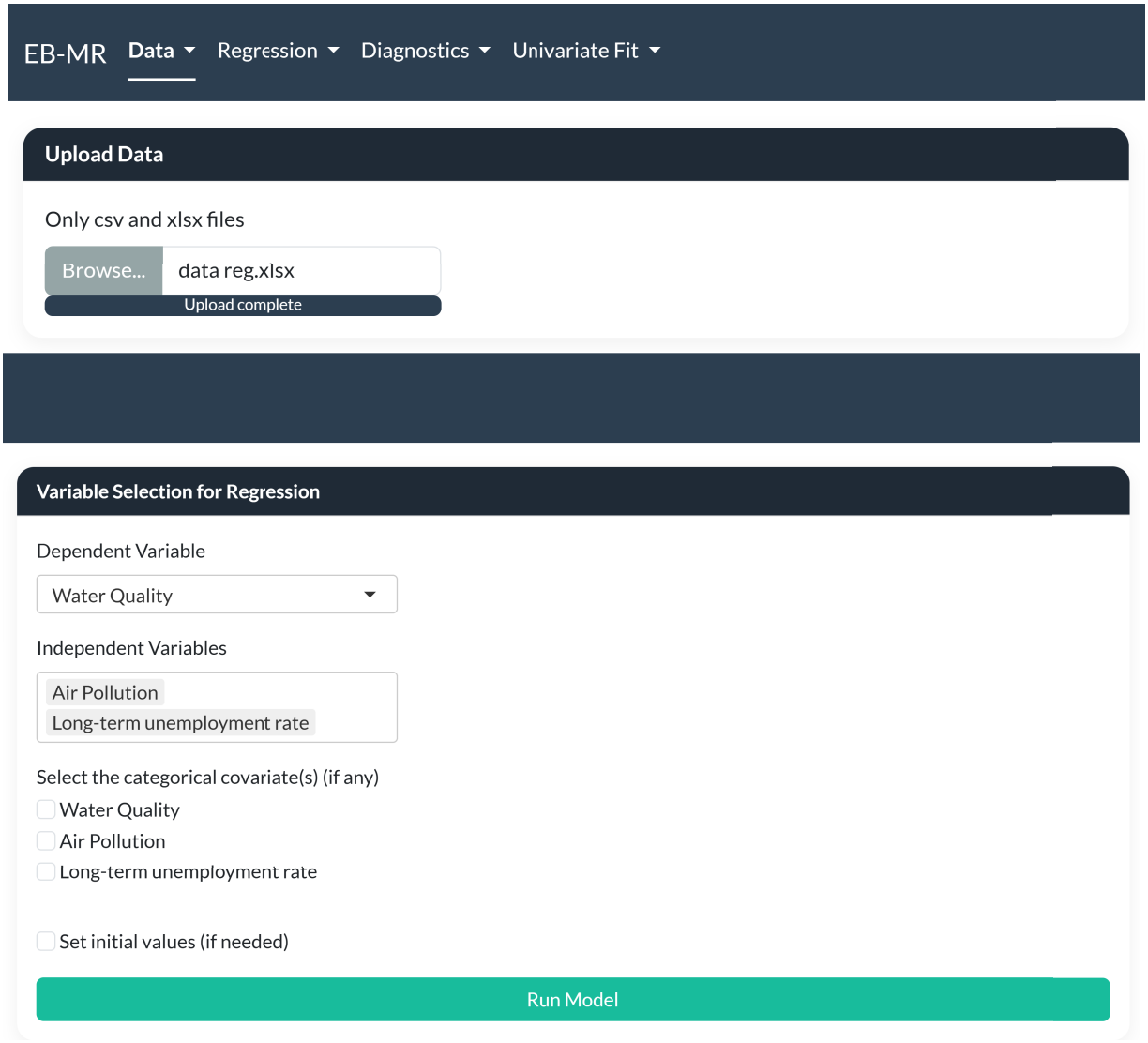


Figure 7: Data upload and variable selection panel.

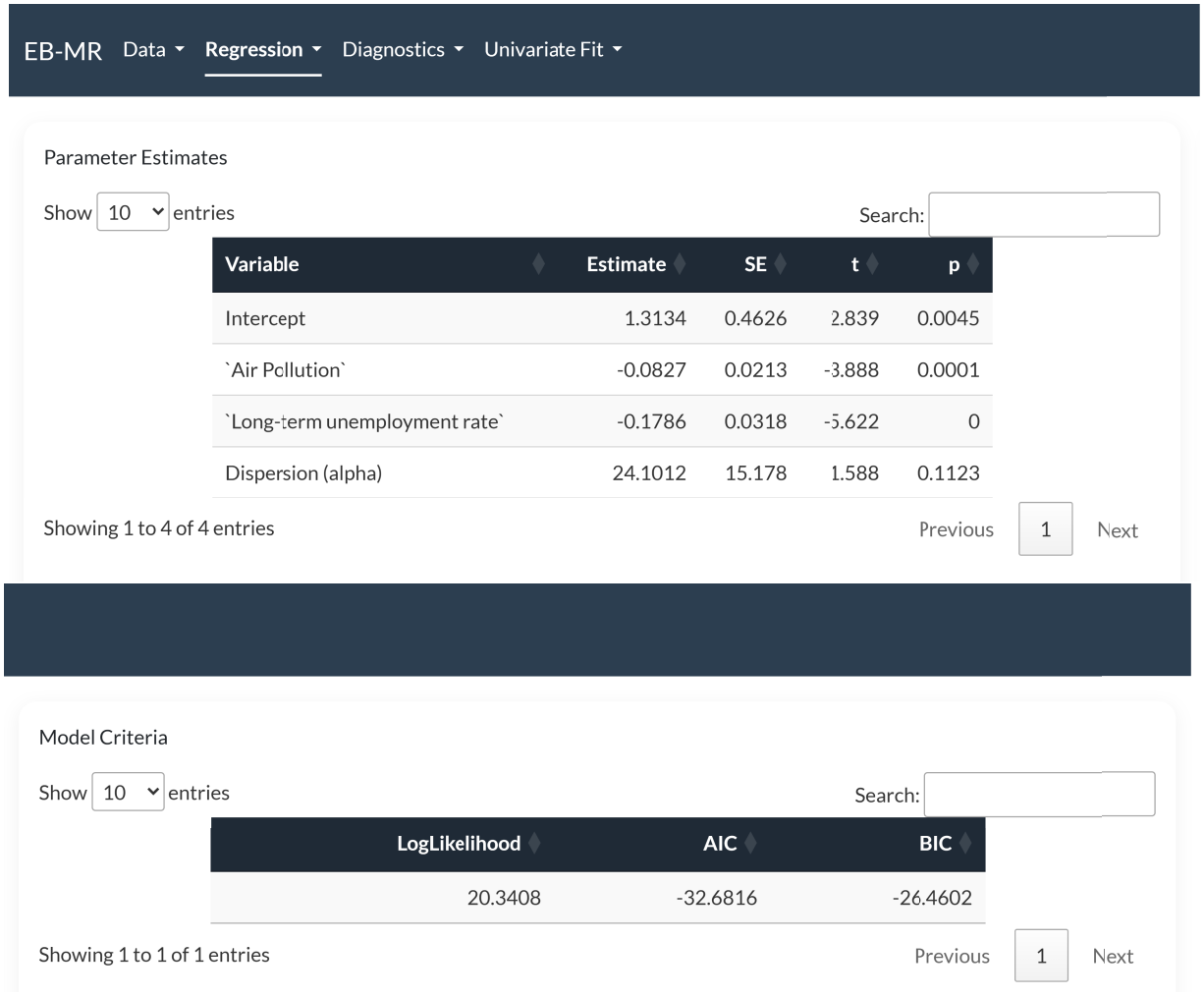


Figure 8: Regression panel.

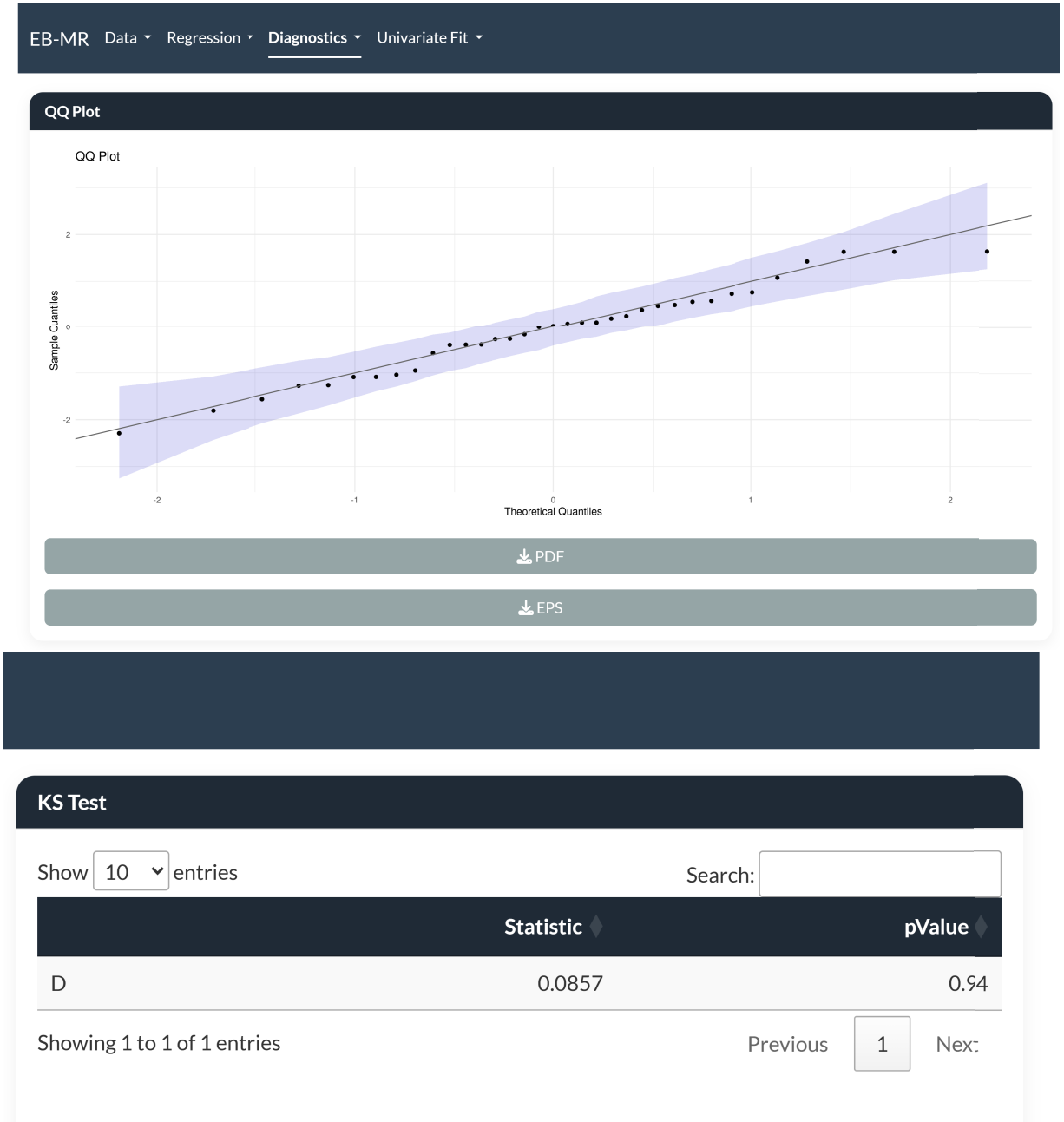


Figure 9: Diagnostics panel.

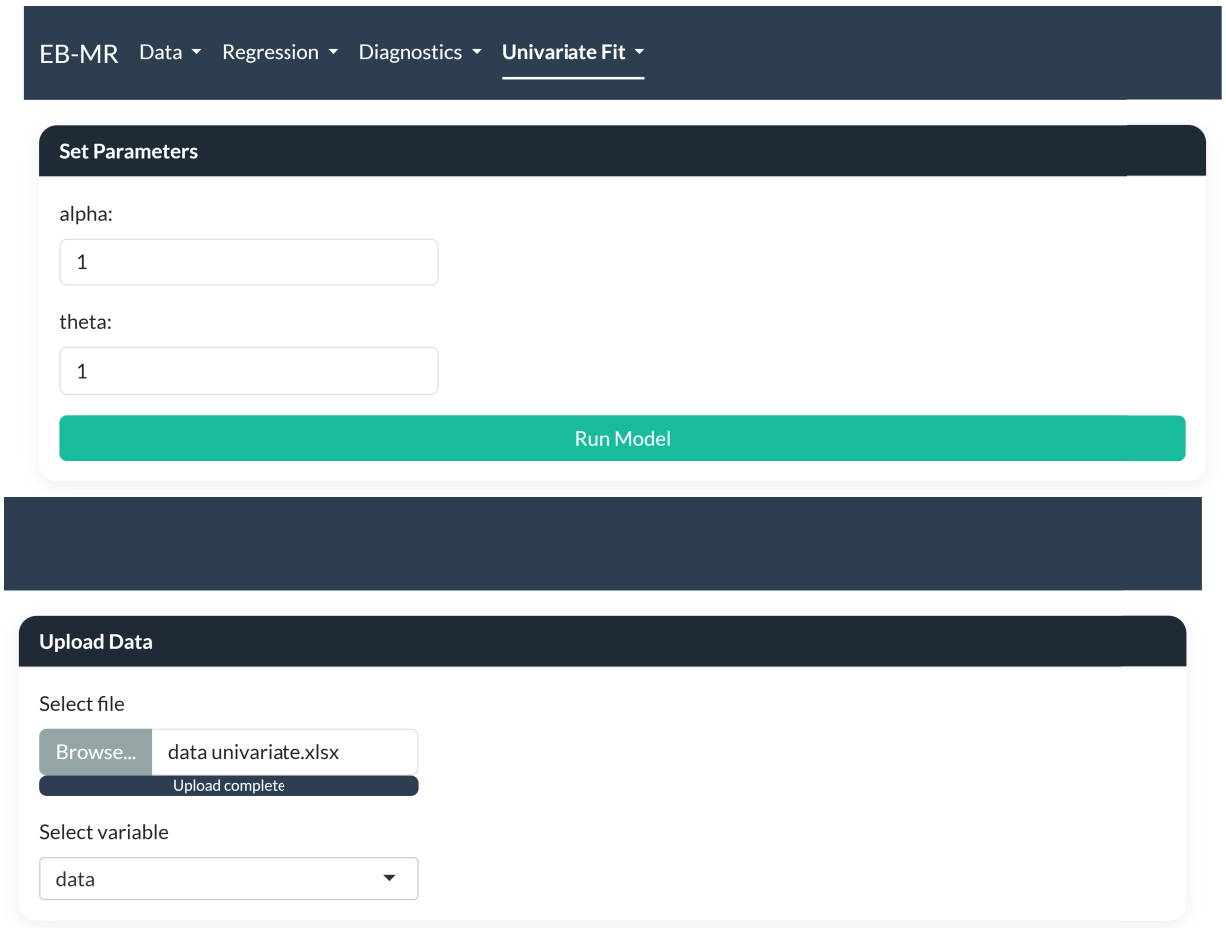


Figure 10: Univariate data fitting panel.

7 Conclusion and Limitations

In this study, a new bounded distribution, referred to as the EB distribution, is introduced as a flexible extension of the classical Bradford distribution. The proposed distribution incorporates an additional shape parameter, allowing it to capture a wide range of distributional behaviors, including various forms of skewness and hazard rate structures. Its structural properties, as well as its connection with the beta distribution, make it both theoretically and practically convenient. A key advantage of the EB distribution lies in the availability of an explicit expression for the mode, which makes it suitable for modal regression modeling. Building on this property, a modal regression framework is developed, enabling the modeling of conditional modes through a parametric and interpretable structure. The estimation procedures based on maximum likelihood are shown to be consistent and efficient as the sample size increases. The practical utility of the EB distribution and its associated regression model is demonstrated through real data applications. The results indicate that the proposed model provides improved fit and greater flexibility compared to several well-known alternatives. In addition, the implementation of the model through an interactive R Shiny application enhances its accessibility in applied research.

Although the EB distribution is flexible and analytically tractable, the distribution has some limitations. First, the numerical optimization required for MLEs may become computationally difficult for large-scale

applications. The proposed model is currently developed for observed bounded response variables and does not directly accommodate censored or truncated data structures that are common in survival and reliability studies. Additionally, the modal regression is studied only for low-dimensional settings, and extensions to high-dimensional covariate spaces may require regularization or penalized estimation techniques. Overall, the EB distribution offers a valuable contribution to the class of bounded distributions and modal regression methodology. Future research may focus on extending the proposed framework to more complex settings such as variable dispersion models, comparison of alternative link functions, or robust estimation techniques.

Acknowledgement: Not applicable.

Funding Statement: The authors received no specific funding for this study.

Author Contributions: The authors confirm contribution to the paper as follows: Conceptualization, Emrah Altun, Christophe Chesneau, Atacan Erdis; methodology, Emrah Altun, Christophe Chesneau, Atacan Erdis; software, Emrah Altun, Christophe Chesneau, Atacan Erdis; validation, Emrah Altun, Christophe Chesneau, Atacan Erdis; investigation, Emrah Altun, Christophe Chesneau, Atacan Erdis; writing—original draft preparation, Emrah Altun, Christophe Chesneau, Atacan Erdis; writing—review and editing, Emrah Altun, Christophe Chesneau, Atacan Erdis; visualization, Emrah Altun, Christophe Chesneau, Atacan Erdis. All authors reviewed and approved the final version of the manuscript.

Availability of Data and Materials: The data supporting the findings of this study are available from the corresponding author upon reasonable request.

Ethics Approval: Not applicable.

Conflicts of Interest: The authors declare no conflicts of interest.

References

1. Sager TW, Thisted RA. Maximum likelihood estimation of isotonic modal regression. Ann Statist. 1982;10(3):690–707. doi:10.1214/aos/1176345865.
2. Collomb G, Hardle W, Hassani S. A note on prediction via estimation of the conditional mode function. J Stat Plan Inference. 1986;15:227–36. doi:10.1016/0378-3758(86)90099-6.
3. Zhou H, Huang X, Alzheimer's Disease Neuroimaging Initiative. Parametric mode regression for bounded responses. Biom J. 2020;62(7):1791–809. doi:10.1002/bimj.202000039.
4. Liu Q, Huang X, Zhou H. The flexible gumbel distribution: a new model for inference about the mode. Stats. 2024;7(1):317–32.
5. Liu Q, Huang X, Bai R. Bayesian modal regression based on mixture distributions. Comput Stat Data Anal. 2024;199:108012. doi:10.1016/j.csda.2024.108012.
6. Wang X, Chen H, Cai W, Shen D, Huang H. Regularized modal regression with applications in cognitive impairment prediction. Adv Neural Inf Process Syst. 2017;30:1448–58.
7. Menezes AF, Mazucheli J, Chakraborty S. A collection of parametric modal regression models for bounded data. J Biopharm Stat. 2021;31(4):490–506. doi:10.1080/10543406.2021.1918141.
8. Hassan AS, Metwally DS, Elgarhy M, Semary HE, Faal A, Mohamed RE. Sine power unit inverse lindley model: Bayesian analysis and practical application. Eng Rep. 2025;7(6):e70242.
9. Muhammad M, Abba B, Xiao J, Alsadat N, Jamal F, Elgarhy M. A new three-parameter flexible unit distribution and its quantile regression model. IEEE Access. 2024;12(149):156235–51. doi:10.1109/access.2024.3485219.
10. Elgarhy M, Abdalla GSS, Hassan AS, Almetwally EM. Bayesian and non-bayesian analysis of the novel unit inverse exponentiated Lomax distribution using progressive censoring schemes with optimal scheme and data application. Comput J Math Stat Sci. 2025;5(1):78–108. doi:10.21608/cjmss.2025.374277.1151.

11. Ghosh I. Bradford distribution and its application in modeling medical data: a suitable alternative to distributions defined on the unit interval. J Appl Stat. 2026;53(3):520–36. doi:10.1080/02664763.2025.2520342.
12. Whittaker ET, Watson GN. A course of modern analysis. Cambridge mathematical library. 4th ed. Cambridge, UK: Cambridge University Press; 2020.
13. Dunn PK, Smyth GK. Randomized quantile residuals. J Comput Graph Stat. 1996;5(3):236–44. doi:10.1080/10618600.1996.10474708.
14. Nasiru S, Chesneau C, Ocloo SK. The log-cosine-power unit distribution: a new unit distribution for proportion data analysis. Decis Anal J. 2024;10:100397.
15. Krishna A, Maya R, Chesneau C, Irshad MR. The unit Teissier distribution and its applications. Math Comput Appl. 2022;27(1):12. doi:10.3390/mca27010012.
16. Korkmaz MC, Chesneau C, Korkmaz ZS. Transmuted unit Rayleigh quantile regression model: alternative to beta and Kumaraswamy quantile regression models. Univ Politeh Buchar Sci Bull Ser Appl Math Phys. 2021;83(3):149–58.
17. Topp CW, Leone FC. A family of J-shaped frequency functions. J Am Stat Assoc. 1955;50(269):209–19. doi:10.1080/01621459.1955.10501259.
18. Bakouch HS, Hussain T, Tosic M, Stojanovic VS, Qarmalah N. Unit exponential probability distribution: characterization and applications in environmental and engineering data modeling. Mathematics. 2023;11(19):4207.
19. Ribeiro TF, Pena-Ramirez FA, Guerra RR, Cordeiro GM. Another unit Burr XII quantile regression model based on the different reparameterization applied to dropout in Brazilian undergraduate courses. PLoS One. 2022;17(11):e0276695. doi:10.1371/journal.pone.0276695.
20. Kumaraswamy P. A generalized probability density function for double-bounded random processes. J Hydrol. 1980;46(1–2):79–88. doi:10.1016/0022-1694(80)90036-0.